Heliyon 9 (2023) e15753

Contents lists available at ScienceDirect

Heliyon

journal homepage: www.cell.com/heliyon

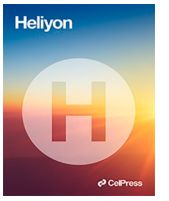

Research article

Process analytical technology as in-process control tool in semi-continuous manufacturing of PLGA/PEG-PLGA microspheres

Arfidin Anwar [a], Pengfei Sun [b], Xiaoxu Rong [b], Abdulaziz Arkin [a], Aliya Elham [a], Zilala Yalkun [c], Xun Li [d,*], Mubarak Iminjan [a,**]

[a] Department of Pharmaceutics and Physical Chemistry, College of Pharmacy, Xinjiang Medical University, Urumqi, 830017, China
[b] University of Wisconsin-Madison, Department of Educational Psychology, Madison, USA
[c] College of Pharmacy, Dalian Medical University, Dalian, 116000, China
[d] Chinese Academy of Science, Department of Chemical Engineering, Beijing, 100190, China

ARTICLE INFO

Keywords:
Continuous manufacturing
mPEG-PLGA/PLGA, process analytical technology
In-process control
And real-time monitor

ABSTRACT

Nowadays, among 3rd generation drug delivery systems, biodegradable polymeric based long-acting injectable depot has achieved tremendous success in clinical application. So far, there have been two dozen of commercial products of Poly (lactic-co-glycolic acid) microspheres available in the market. Recently, continuous manufacturing concept has been successfully applied on oral solid formulation from buzzword to reality. However, the polymeric injectable microspheres are still stayed at batch manufacturing phase due to the lack of understanding of knowledge matrix. In this study, micro-mixer as a plug-and-play emulsification modules, Raman spectroscopy and focused beam reflectance measurement as real-time monitoring modules are integrated into a novel semi-continuous manufacturing streamline to provides more efficient upscaling flexibility in microspheres production. In this end to end semi-continuous manufacturing process, amphiphilic block polymer monomethoxy-poly (ethylene glycol) modified PLGA (mPEG-PLGA) was used for encapsulating Gallic acid. Additionally, with guarantee of good robustness, the correlation relationship between critical process parameters, critical material attributes and critical quality attributes were investigated. The time-space evolution process and mechanism for formation of PEG-PLGA microsphere with particular morphology were elaborated. Altogether, this study firstly established semi-continuous manufacturing streamline for PLGA/PEG-PLGA microspheres, which would not only lower the cost of production, narrow process variability and smaller equipment/environmental footprint but also applied in-process control (IPC) and QbD principle on complicated production process of microspheres. Therefore, this study build confidence in the industrial development of PLGA/PEG-PLGA microspheres and establish best practice standards, which might be a quantum leap for developing PLGA microspheres in the future.

1. Introduction

Poly (lactic-co-glycolic acid, PLGA) microspheres as long-acting injectable have achieved tremendous success since 1986 when the

* Corresponding author.
** Corresponding author.
E-mail addresses: lixun@ucas.ac.cn (X. Li), Z2212038@xjmu.edu.cn (M. Iminjan).

https://doi.org/10.1016/j.heliyon.2023.e15753
Received 7 November 2022; Received in revised form 18 April 2023; Accepted 21 April 2023
Available online 23 April 2023

first commercial PLGA microspheres product (Decapeptyl® 3.75 mg from Ferring pharmaceuticals) was approved by European Medicines Agency [1,2]. Due to its tunable biodegradation duration and outstanding biocompatibility, the marketing performance of PLGA based formulation exhibited strong potential prospects [3–5]. However, till date, the quality by design (QBD) principles has not been applied on PLGA microspheres development yet [4]. More importantly, the correlation relationship between critical material attributes, critical process parameters and critical quality attributes are ambiguous which severely hinders the development of PLGA microspheres from bench to bedside. Meanwhile.

Recently, with the progressing of Industry 4.0 concept, continuous manufacturing process which defined as the integration of a series of unit operations, processing materials continually to produce the final pharmaceutical product has been strongly prompted by FDA [6–10]. Compared with traditional batch manufacturing process, continuous manufacturing eliminates the need for off-line testing and storage, thereby reducing the number of manufacturing steps. Therefore, there are various benefits of continuous manufacturing approach, included higher production efficiency, enable saving labor and warehouse space, reducing processing and holding time and better robustness [11–14]. More importantly, with the introduction of process analytical technology (PAT) into continuous manufacturing [15], highly automated processes could be facilitated, and better understanding of process could be gained [2,8,9,16,17]. However, because of the relatively complicated preparation process, there is still lack of study focused on applying continuous manufacturing on polymeric based microspheres [18–22].

In this study, mPEG-PLGA, an amphiphilic block copolymer was selected as polymer matrix [23–26], meanwhile, gallic acid, a small molecule compound with potential for anticancer activity was used as model drug [27–29]. Micro-mixer with high production efficiency based on the mechanism of flow chemical system was used for microspheres preparation. Meanwhile, a 'plug-and-play' emulsification operation unit of Raman spectroscopy [30,31] and focused beam reflectance measurement [32–34] as real-time monitoring modules are integrated into this semi-continuous microspheres manufacturing streamline to monitor the dynamic trend of solidification process. Moreover, full and systematically characterization include encapsulation efficiency, yield, in-vitro release, particle size distribution, surface morphology, internal structure, porosity, thermo dynamic study were performed. Subsequently, the emulsion-microspheres evolution mechanism was elaborated by investigating solidification dynamic. Altogether, building this semi-continuous manufacturing streamline not only lower the cost of production, reduce process variability and smaller equipment/environmental footprint but also applied in-process control and QbD principle on complicated production process of microspheres [35,36]. Therefore, this study build confidence in the industrial development of PLGA/PEG-PLGA microspheres and establish best practice standards, which might be a quantum leap for developing PLGA microspheres in the future.

2. Materials and methods

2.1. Materials

Gallic acid (*LOT: C11987271*) and gallic acid reference substance (*LOT: C12211933*) were purchased from *Macklin, Shanghai, China*, mPEG(1K)-PLGA(19K, LA/GA = 50/50) copolymer was purchased from *Jinan DaiGang Biotechnology Co., Ltd. (Stored at -20°C), Jinan, Shandong, China*, poly-vinyl alcohol (PVA)(*LOT:2190203*) was purchased from *Jiangxi Alpha Hi-tech Pharmaceutical Co., Ltd., Jiangxi, China*, sodium chloride (*LOT: X22E048*) was purchased from *Alfa Aesar, Shanghai, China*. 85% phosphoric acid (*LOT: A0400969*) and acetonitrile (ACN, *LOT: 213447*) were purchase from *Thermo-fisher, Shanghai, China*, dichloromethane (DCM, *LOT: 4503599052*) was purchased from *sigma-Aldrich, USA*. 85% phosphoric acid, ACN, DCM were all analytical pure and used directly.

2.2. Experimental equipment

MS205DU precision electronic balance used for weighting, ParticleTrack™ G400 focused beam reflectance measurement (FBRM) Particle size analyzer used for Monitoring the change of microsphere size during solidification (*Mettler Toledo, America*), KAISER Raman Rxn 2 used for Raman spectrum (Analytic Jena, Germany), RCT B S025 magnetic stirrer used for solidification (*IKA company of Germany*), VALVE MIXER 30 Micro-reactor system used for manufacturing microspheres (*EHRFELD, Germany*), free zone triad lyophilizer used for dry-frozen microspheres (*Labcono, USA*), 97043-954 Ultrasonic cleaning machine (VWR, USA), 5430 high-speed centrifuge (*Eppendorf, Germany*), sw23-40 water bath pot used for *in-vitro* release (*Julabo, Germany*), phenom pure scanning electron microscope used for microspheres morphology test (SEM, *Thermo Fisher, USA*), Mastersizer 3000 laser granulometry used for measurement of microspheres particle size (*Malvern, UK*) SP5 Laser scanning Confocal Microscopy used for microspheres morphology test (*Leica, Germany*), Acquity ultra high performance liquid chromatograph (*waters, America*), Novagen® D-tube™ dialyzer maxi, MWCO 12–14 kDa (Merck, USA)RO 613l reverse osmosis pure water machine (*sartorius, Germany*), TA-XT plus 100 Stable Micro System's Texture analyzer used for injectability test (*Texture technologies Corporation, UK*), Discovery25 Differential Scanning Calorimeters used for DSC test (*TA instrument, USA*), 1 mL LS 25 GA 5/8 sterile syringe (BD, USA).

2.2.1. Preparation of mPEG-PLGA microsphere

Briefly, gallic acid was dissolved in distilled water with concentration of 5% (m/v) and heated at 70 °C in a water bath until completely dissolved and then gallic solution was use as drug phase. mPEG-PLGA was dissolved in dichloride methane (DCM) with a concentration of 15%, 25% and 35%(w/v) as polymer phase. At the same time, poly(vinyl-alcohol) (PVA) was dissolving in distilled water with a concentration of 0.5%, 1% and 2% (w/v) for 3 h at 50 °C and saturated with 1.15% (w/v) gallic acid as surfactant phase.

The semi-continuous manufacturing streamline for PLGA/mPEG-PLGA microspheres was shown in Fig. 1. Two mixers included LH mixer and valve assisted mixer are used for emulsification in this system. Thereinto, micro-mixer system with two-step emulsification

process was firstly used for the preparation of PLGA microspheres. In this study, LH mixer was used for the formation of primary emulsion, while valve-assisted mixer was used for the formation of secondary emulsion. This is because the stability of primary emulsion could be improved by decreasing the droplet particle size. Compare with valve assisted mixer, LH mixer with higher shear force is suitable for producing emulsion droplets with smaller particle size. Polymer phase and drug phase were fed by HPLC pumps with flow rate of 20 mL/min and 5 mL/min, respectively. After feeding into LH2 mixer equipped with 150/50 μm mixing plate and 50 μm aperture plate, the W/O primary emulsion with smaller particle size were formed. Then the surfactant phase fed by mechanic pump with 200 mL/min was mixed with primary emulsion in valve-assisted mixer to form W/O/W secondary emulsion. Subsequently, solidification process was performed under room temperature and ambient condition. During the solidification process, the process analytical technology (PAT), including Raman spectroscopy and particle size analyzer were used for the monitoring the real-time trend of PLGA conc, residual solvent conc and particle size and identifying endpoint of solidification process.

Then regular washing procedure was performed by centrifuge under 5000 g of centrifugal force. After 5 times of washing by pure water, the samples were collected into 1 tube for freeze-drying.

2.3. Surface morphology observation

The microsphere powder was evenly adhered to the conductive adhesive, and the conductive adhesive was adhered to the sample table. The gold was sprayed twice at 150 mA current for 5s under vacuum and observed by SEM by 20 kV accelerating voltage.

2.4. Encapsulation efficiency% measurement

GA loaded microspheres (25 mg) were added with 2 mL acetone, add appropriate amount of methanol, sonicated for 30 min, add methanol to 50 mL, sonicate for 15 min, centrifuged at 7800 rpm for 5min, and the supernatant was taken for UPLC test and calculated GA concentration by calibration curve of $y = 47597x - 58840$ ($R^2 = 0.9991$).

The concentration of gallic acid was determined by ultra-performance liquid chromatography (UPLC) using a waters C18 (100 mm × 2.1 mm × 1.7 μm) column assay. Elution was performed at 0.2% aqueous phosphoric acid/methanol = 83/17 with a flow rate of 0.12 mL/min and UV absorbance at 273 nm. The drug loading efficiency (LE%) and encapsulation efficiency (EE%) of microspheres are calculated by the following equation:

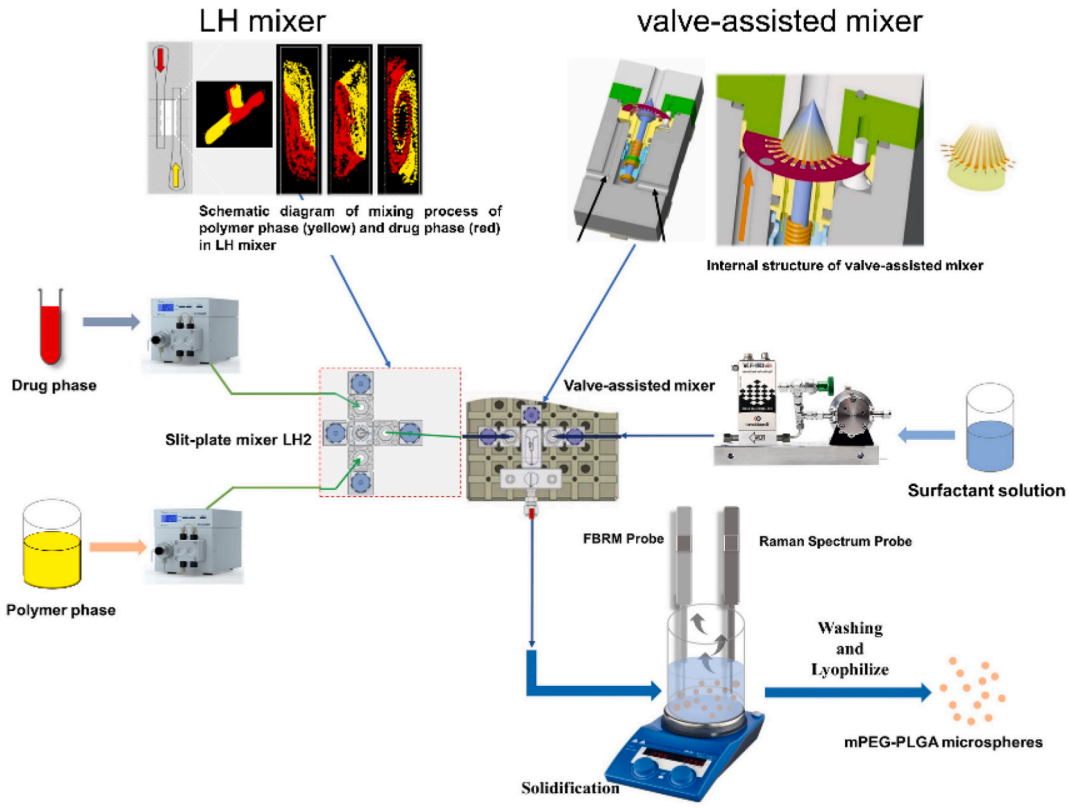

Fig. 1. Schematic illustration of mPEG-PLGA microspheres using microfluidics process.

$$LE\% = \frac{a}{b} \times 100\% \quad (1)$$

where, b is the total weight mass of the microspheres (including the loading mass of polymer and GA), and a is the loading mass of GA in the microspheres which measured by UPLC method. LE% indicated the actual drug loading after microspheres preparation method.

$$EE\% = \frac{m}{m_0} \times 100\% \quad (2)$$

Encapsulation efficiency refers to the amount of drug loaded by a unit weight or a unit volume of microspheres. Where m_0 is the total mass of GA added and m is the mass of GA loaded in the microspheres which measured by UPLC method.

All data are processed with Origin.

2.5. In-vitro cumulative release behavior

Accurately weight 20 mg of GA loaded mPEG-PLGA microspheres into D-tube™ membrane, add 1 mL of phosphate buffer saline (PBS) containing 0.04% benzalkonium, 0.1% tween 20 and 0.5% L-Cysteine hydrochloride, put the D-tube™ into a 50 mL centrifuge tube and add 25 mL PBS media under agitation at 37 °C. Supernatants were collected at predetermined intervals and replaced with fresh PBS media of equal volume. The concentration of gallic acid was determined by ultra-performance liquid chromatography (UPLC) using a waters C18 (100 mm × 2.1 mm × 1.7 μm) column assay. Elution was performed at 0.2% aqueous phosphoric acid/methanol = 83/17 with a flow rate of 0.12 mL/min and UV absorbance at 273 nm. All the release experiments were executed in triplicate. All data are processed with Prisim.

2.6. Determination of specific surface area and particle size

Sufficient weight of lyophilized microspheres was loaded into the sample tube, add an appropriate volume of distilled water to resuspend it. Drop the microsphere suspension into the sample pool of the particle size analyzer, disperse the suspension evenly in the sample pool at 1500 rpm, and measure the particle size, specific surface area. All data are processed with Prisim.

2.7. Particle size distribution change trend monitored by FBRM

Particletrack™ with Focused Beam Reflectance Measurement (FBRM) Technology was used for monitoring particle size change trend during the solidification process. The FBRM 19 mm probe was inserted under emulsion surface approximately 3 cm below. The frequency of detection timepoint was set as 5 min. All data are processed with Origin.

2.8. Organic solvent content, PVA concentration and polymer concentration trend monitored by Raman spectroscopy

With the organic solvent, in this case, DCM evaporation, polymer start to precipitate and encapsulate API during the solidification process. Therefore, the dynamic change of solidification process is super critical [37,38]. In this part, Raman spectrum process analytical technology (PAT) was used for monitoring DCM content, mPEG-PLGA concentration and PVA concentration during the whole solidification process. Firstly, Sliver paper was used for covering solidification container for avoid the interference of environmental illumination. A series concentrations of DCM were 0.15, 0.1, 0.05, 0.03 and 0.02 mg/mL, PVA solution were set as 1.997, 1.49775, 0.9985, 0.49925 and 0.249625 mg/mL and mPEG-PLGA were set as 250.683, 200.5464, 100.2732, 50.1366 and 25.0683 mg/mL. All these substances were prepared for establishing Raman spectra multivariate linearity models.

250 cm^{-1}–3500 cm^{-1} wavelength scan was performed for each substance. After achieving full wavelength by GRAMS suite spectral processing software, specific shift and region for each substance was identified and recorded in the software. Then after simulation and calculation, linearity models for each substance were achieved. During the solidification process, the Raman spectrum probe was inserted approximately 3 cm below the liquid surface of the emulsion, data were collected and recorded every 5 min.

2.9. Injectability test of microspheres

The injectability of microspheres was tested with Texture analyzer. Take approximately 10 mg mPEG-PLGA-MS into a 2 mL centrifuge tube. Use a 1 mL syringe to add 1 mL saline. After suspension, use a 1 mL syringe to take out 0.35 mL of microsphere suspension. Place the syringe in Texture analyzer. Beat out the suspension at a speed of 2.00 mm/s and a pressure of 49 N. All data are processed with Origin.

2.10. Differential scanning calorimetry (DSC) test

5 mg Weigh and take about 5 mg of samples into Tzero aluminum pan, including reference, mPEG-PLGA blank microspheres, mPEG-PLGA microspheres loaded with GA, gallic acid monomer, mPEG-PLGA, GA and mPEG-PLGA physically mixed. The test temperature is 10 °C–350 °C, and the heating rate is 10 °C/min. All data are processed with Origin.

3. Result and discussion

3.1. Identification of critical material attributes and critical process parameters

In this study, since this is the first time using micro-mixer as semi-continuous manufacturing tool for polymeric based microspheres development, the optimization process, especially critical material attributes and critical process parameters have been never identified before. Therefore, di-block copolymer PEG-PLGA was used as microspheres matrix instead of PLGA [39]. Because of its amphiphilic property, using PEG-PLGA is less easily to induce blockage of aperture/mixing plate of micro-mixer during the polymer precipitation process, even at a high concentration of polymer phase. The optimization process could be found in Tables 1 and 2.

It could be easily found that the critical factor in micro-mixer preparation approach is input energy which determined by feed rates of drug phase, polymer phase and surfactant phase. In the meantime, all groups (F1–F6) exhibited narrow particle size distribution which is an additional benefit of micro-mixer. Moreover, with the feed rate increased, the particle size became smaller. Considering the encapsulation efficiency, the best ratio of drug phase, polymer phase and surfactant phase is 5:20:200 (mL/min). Obviously, the emulsification mechanism for micro-mixer is quite different from that of ($W_1/O/W_2$) double emulsion method [40–42]. Compared with traditional preparation method of ($W_1/O/W_2$) double emulsion method, the micro-mixer approach required less volume of polymer phase and surfactant phase, which would reduce cost significantly. From F1–F6, we can fount that, the encapsulation efficiency determined by the ratio of drug phase to polymer phase. Increase the feed rate of polymer phase could increase the encapsulation efficiency. This is because the stability of primary emulsion droplet is important for the encapsulation process. Therefore, increasing the feed rate of polymer phase could decrease the particle size of primary emulsion droplet which result in improving the stability of the primary emulsion droplet. However, when the feed rate of polymer phase comes to 30 mL/min, the encapsulation decreased due to the leakage of drug caused by the intense mixing condition. In terms of the feed rate of surfactant phase, the higher rate led to a higher encapsulation efficiency. Because the higher feed rate of surfactant phase decreases the oil/aqueous interfacial tension that prevent the drug escape phenomenon. After primary optimization process, the optimal parameters were exhibited in Batch No. F4. Therefore, subsequent formula optimization process were conducted based on F4's process parameters.

Polymer phase concentration and surfactant phase concentration have been optimized as Table 2 shown. From F4, F7 and F8, it could be found that with the increase of polymer phase concentration, the encapsulation efficiency increased. This is because the higher concentration in polymer phase led to a higher viscosity which would prevent the drug to escape out during the emulsification process. Additionally, trend could be found from F7, F9 and F10, with the surfactant phase concentration increased from 0.5% to 2%, the encapsulation efficiency decreased. Interestingly, it is an opposite trend with that in ($W_1/O/W_2$) double emulsion method. This is because the emulsification mechanism is different. In traditional double emulsion method, the input energy is relatively low. Therefore, surfactant such as PVA, poloxamer was mainly used as emulsifier for decreasing interfacial tension and stabilizing emulsion. However, in micro-mixing approach, the input energy is higher. Therefore, excess surfactant would generate air bubble which reduce emulsification effect. Altogether, F7 was chosen as the optimal formulation for the systematic characterization.

3.2. Surface morphology and internal structure

The surface morphology was observed by scan electron microscope and meanwhile, laser scanning confocal microscope was used for observing internal structure of GA loaded PEG-PLGA microsphere (F7). As Fig. 2A and B shows, irregular winkle-like of surface morphology was found. Additionally, the internal structure of GA loaded PEG-PLGA were shown as Fig. 2C. Obviously, the porous internal structure was exhibited. As Fig. 2D–F shows, compared with the smooth surface and solid internal structure normally observed in PLGA microspheres, the surface morphology and internal structure are quite different. This distinction is mainly caused by the inherent properties of polymer. Because the PEG-PLGA is amphiphilic, it would lead to a different solidification process which result in the particular surface morphology and internal structure.

Table 1
Process parameters of GA loaded PEG-PLGA microspheres.

Batch No.	Feed rate of drug phase (mL/min)	Feed rate of polymer phase (mL/min)	Feed rate of surfactant phase (mL/min)	Actual Drug loading %	Encapsulation efficiency %	Particle size (um)	Span (PSD)	Initial burst release (0–4 h)
F1	5	10	100	1.72 ± 0.23	44.67 ± 0.55	23.62 ± 0.48	0.826 ± 0.56	6.83% ± 1.98
F2	5	10	200	2.7 ± 0.51	70.13 ± 0.67	19.38 ± 0.51	0.738 ± 0.53	8.26% ± 2.06
F3	5	20	100	1.93 ± 0.37	50.13 ± 0.28	20.81 ± 0.69	0.711 ± 0.34	12.94% ± 2.58
F4	5	20	200	3.36 ± 0.22	87.27 ± 0.34	16.37 ± 0.45	0.737 ± 0.29	15.27% ± 1.72
F5	5	30	100	2.09 ± 1.03	54.28 ± 2.55	17.31 ± 0.73	0.839 ± 0.78	14.13% ± 2.97
F6	5	30	200	2.96 ± 0.94	76.82 ± 2.39	12.38 ± 0.64	0.836 ± 0.64	32.16% ± 1.45

*Each sample was manufactured in triplicated; Each sample was tested in triplicated.

Table 2
Formulation parameters of GA loaded PEG-PLGA microspheres.

Batch No.	Polymer phase concentration (mg/mL)	Surfactant phase concentration (w/v%)	Actual Drug loading %	Encapsulation efficiency %	Particle size (um)	Span (PSD)	Initial burst release (0–4 h) %
F4	150	0.5	3.36 ± 0.22	87.27 ± 0.34	16.37 ± 0.45	0.737 ± 0.29	15.27% ± 1.72
F7	250	0.5	3.52 ± 0.33	91.42 ± 0.47	18.51 ± 0.63	0.781 ± 0.66	10.04 ± 1.58
F8	350	0.5	3.57 ± 0.37	92.72 ± 0.53	19.38 ± 0.51	0.883 ± 0.43	3.12 ± 2.33
F9	250	1	3.12 ± 0.29	81.03 ± 0.39	17.54 ± 0.37	0.744 ± 0.91	11.23 ± 1.98
F10	250	2	2.99 ± 0.21	77.66 ± 0.22	15.27 ± 0.49	0.724 ± 0.52	32.16 ± 1.74

*Each sample was manufactured in triplicated; Each sample was tested in triplicated.

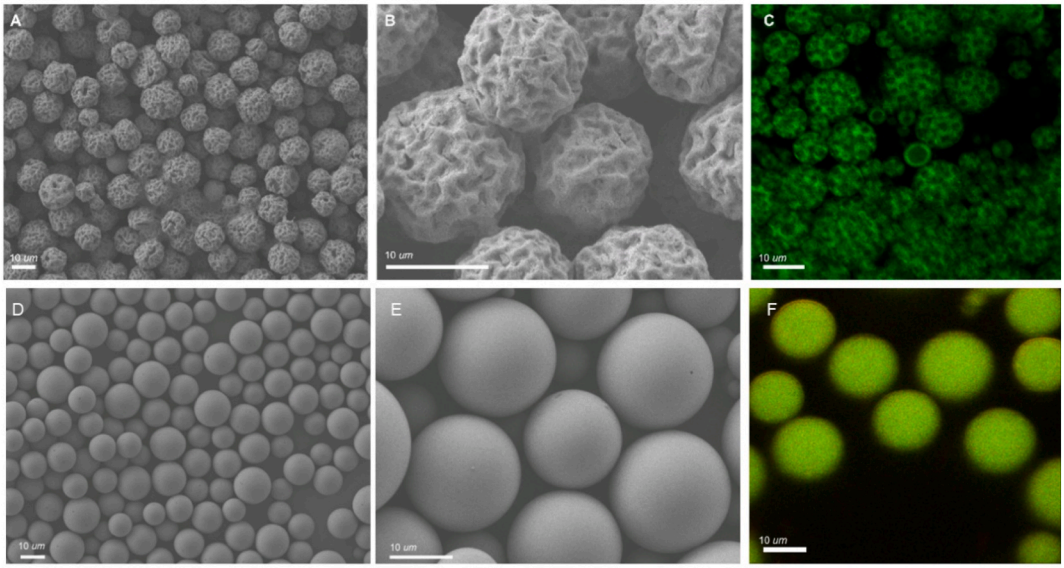

Fig. 2. (A) Surface morphology of F7 by SEM under 1000X, (B) Surface of morphology of F7 by SEM under 5000X, (C) Internal structure of F7 by LSCM under 2500X, (D) Surface morphology of PLGA microspheres by SEM under 1000X, (E) Surface of morphology of PLGA microspheres by SEM under 5000X, (F) Internal structure of PLGA microspheres by LSCM under 2500X

Moreover, the specific surface area and pore size distribution of F7 was measured by laser granulometry method. In this study, the PLGA blank microspheres was set as control group. The results were shown in Fig. 3. It can be seen that the porosity of the mPEG-PLGA microspheres is significantly larger than that of PLGA microspheres. The pore volume of PLGA microspheres is close to 0, indicating that the surface is smooth and there is no pore internal structure. Meanwhile, the porosity of mPEG-PLGA microspheres is relatively high which confirm the SEM results.

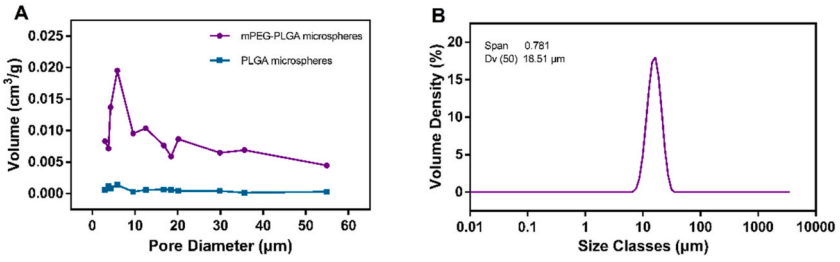

Fig. 3. (A) Pore diameter distribution of mPEG-PLGA microsphere and blank PLGA microsphere, (B) Particle size distribution of mPEG-PLGA microspheres.

3.3. In-vitro release profile

The *in-vitro* release profile of F7 was shown in Fig. 4. It could be found that, the initial burst release of F7 is relatively low, compared with microspheres prepared by mPEG-PLGA. The GA released at a constant rate from 0 h to 12 h, which indicate the dissolution of GA located and distributed in the close surface of microspheres. And from 12 h to 312 h, the release rate was speed up, which reflect the degradation of polymer matrix start. Moreover, from 312 h to 600 h, a plateau was appeared, which represent the diffusion of GA inside of matrix dominated the release behavior. The whole release behavior looks like 0-zero release pattern. However, after 600 h, the total release amount of GA did not reach 100%. Mass balance was conducted to verify the drug lost during the dissolution process. The results showed that there was no existed drug after 600 h. Therefore, the drug degradation might be the main reason.

3.4. Establish of Raman spectrum linearity model of DCM, PVA and mPEG-PLGA with different concentration

As shown in Fig. 5A–C, each individual line indicates one concentration of corresponding substance. Meanwhile, the RAMAN characteristic peaks for DCM, mPEG-PLGA and PVA were identified. In the meanwhile, the linearity regression was established using different concentration for each substance.

The linearity regression parameters of DCM, mPEG-PLGA, and PVA concentrations could be found in Table 3. The R^2 for each substance is >0.999 which indicated good linearity correlation. Hence, the concentration linearity model could be used for concentration monitor and calculation in the solidification process.

3.5. Monitoring of DCM, PVA and mPEG-PLGA concentration with Raman spectrum

The content of organic solvent, surfactant and polymer were monitored during the whole solidification process. The results were shown in Fig. 6A and B. Fig. 5A represented the overall trend of concentration of DCM, PVA and MPEG-PLGA versus time. Fig. 5B summarized the concentration of each substance. With the organic solvent evaporation in solidification process, the DCM concentration decreased, and polymer concentration increased. Moreover, it could be found that, after 90 min, the concentration of DCM and peg-polymer concentration would not change anymore, which indicate that the endpoint of solidification was 90 min. Therefore, with the utilize of Raman spectroscopy, not only the trend of organic solvent, polymer concentration and surfactant content could be monitored, but also the endpoint of solidification process could be determined.

3.6. Monitoring of particle size trend

The particle size change trend during the whole solidification process was monitored by FBRM G400 Particle size analyzer and shown in Fig. 7A. Interestingly, there are three phases of particle size change in the solidification process which are quite different from that of PLGA solidification process Firstly, from 0 min to 120 min, the particle size gradually increased from 25 μm to 28 μm. This is because the hydrophilic chain of PEG stretched to water phase and absorbed water, which led to a larger hydrate particle size Subsequently, from 120 min to 130 min, the particle size significantly dropped, which indicate emulsion droplet turn into microspheres with the evaporation of organic solvent. This is because the amphiphilic property of mPEG-PLGA plays a role as emulsifier which is able to decrease interfacial tension. Because the water molecule combines with peg chain, therefore, the PLGA chain direct to core of emulsion droplet harden faster, after precipitation of PLGA chain, the copolymer lost its amphiphilic property. Moreover, from 130 min to 300 min, the particle size did not change any more which reflects that the solidification process was completed. Therefore, the solidification mechanism was proposed as Fig. 7B. More important, the end point of solidification was determined by monitoring the trend change of particle size.

3.7. Injectability measurement

The injectability of F7 was tested. As Fig. 8 shows, the force range for injecting is between 187.6 and 90.53 g, which indicated a good injectability. In the meanwhile, the relatively higher drug loading would decrease the inject volume which further reduce the

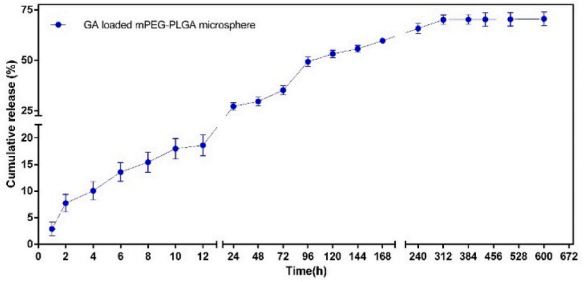

Fig. 4. *In-vitro* release behavior of F7 in 25 days.

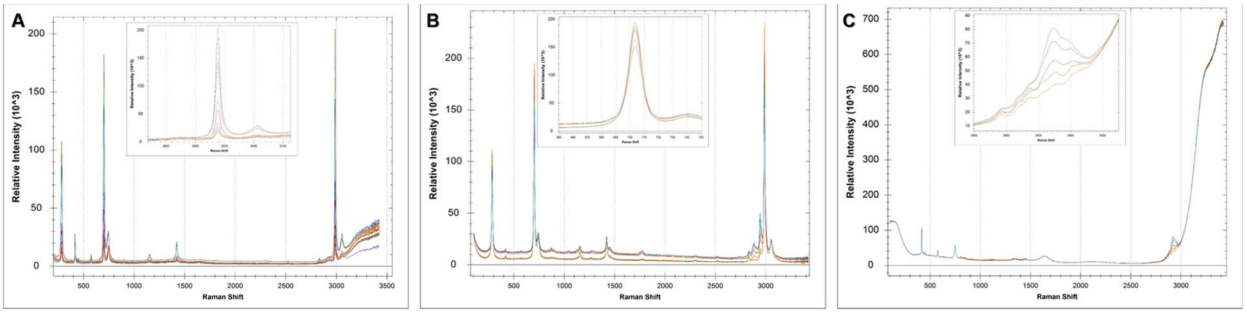

Fig. 5. RAMAN characteristics peaks and substance with different concentrations that used for establishing linearity (A: DCM; B: mPEG-PLGA; C: PVA).

Table 3
Linearity parameters of substance in Raman analysis.

Solution	Intercept	Slope	Pearson's r
mPEG-PLGA	0.11479	0.99948	0.99994
DCM	0.00257	0.98457	0.99970
PVA	0.00407	0.99948	0.99998

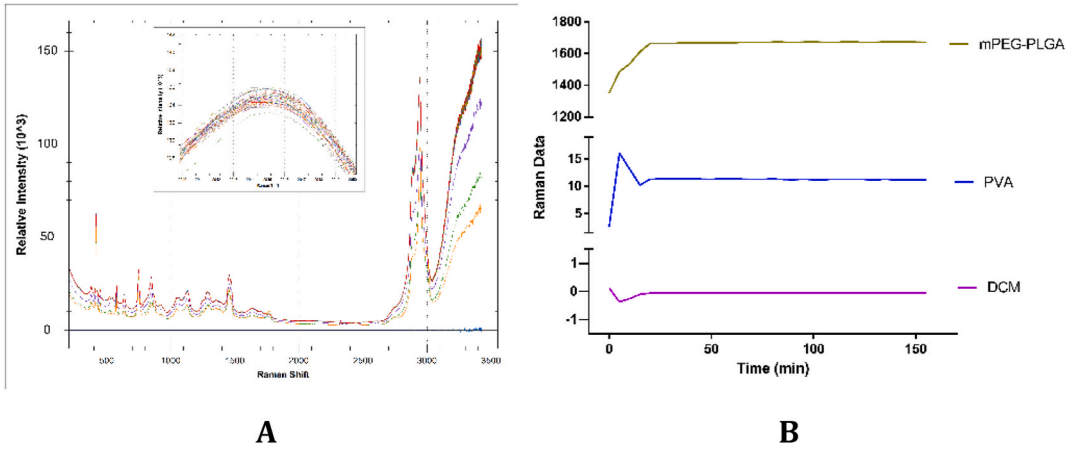

Fig. 6. (A) RAMAN characteristics peaks of dichloromethane, PVA and mPEG-PLGA during solidification, (B) Result of monitoring of the concentration changes of dichloromethane, PVA and mPEG-PLGA during solidification.

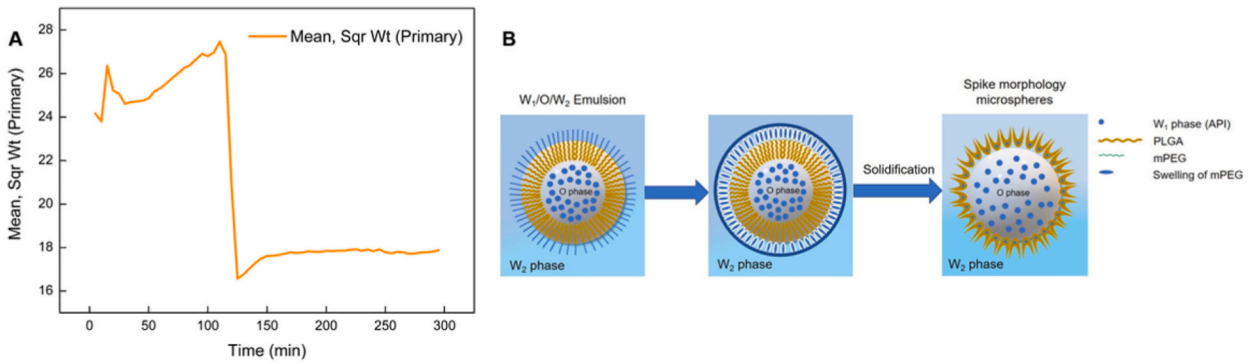

Fig. 7. (A) Trend of particle size change during solidification process, (B) The transform mechanism of emulsion droplet to microspheres.

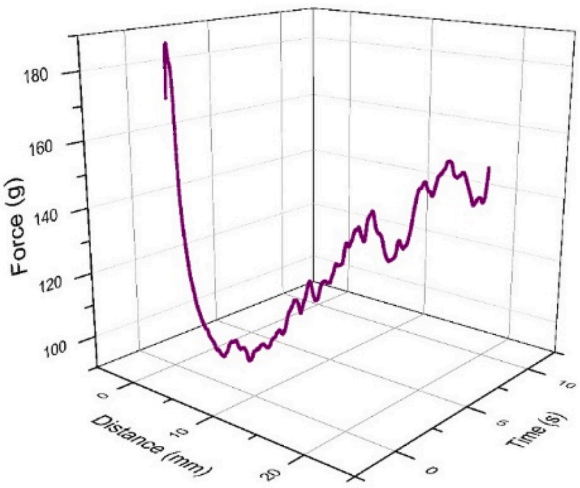

Fig. 8. The injectability of mPEG-PLGA GA loaded microsphere.

pain caused by administration in clinical.

3.8. Differential Scanning Calorimeters (DSC) test

DSC test was performed for investigating the GA and polymer chemical-physical state after encapsulation process. As Fig. 9 shows, there are four groups shown in this study. Gallic acid and mPEG-PLGA as raw material groups, Gallic acid physically mixed with mPEG-PLGA as control groups. And GA loaded mPEG-PLGA microsphere as research group. It could be found that, the encapsulated GA exhibited the same crystal peak with GA raw material group, which reflected the encapsulated GA in microspheres was stayed crystalline state. In the meanwhile, the mPEG-PLGA kept amorphous state consistently after encapsulation process. In short, the GA and polymer did not changed physical state during the encapsulation process, even though undergo a relatively high energy input.

4. Conclusion

In this study, micro-mixing tool combined with process analytical technology were used for manufacturing GA loaded mPEG-PLGA microspheres in continuous manner. Additionally, critical process parameters included phase feed rate, critical material attributes included polymer phase concentration, surfactant phase concentration in micro-mixing technology were investigated. After optimization, mPEG-PLGA microspheres with high encapsulation efficiency (91.42%), narrow particle size distribution (0.781) and low initial burst release (10.04%) was achieved.

In the meantime, process analytical technology was firstly used as real-time in process control tool in microspheres development. RAMAN characterize peak for DCM, polymer and surfactant was identified. Subsequently, linearity regressions with 0.99 of R^2 for

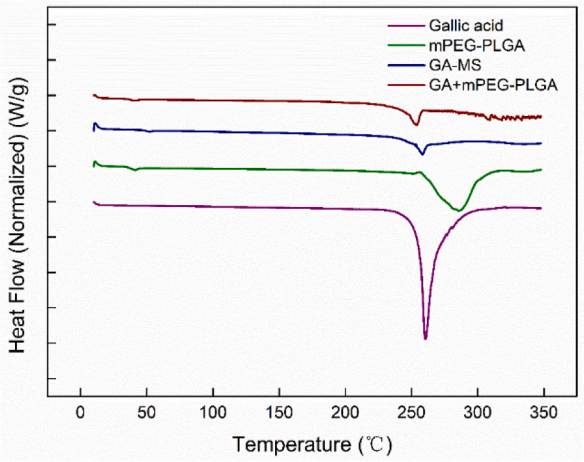

Fig. 9. DSC test of gallic acid, mPEG-PLGA, gallic acid physically mixed with mPEG-PLGA and gallic acid loaded mPEG-PLGA microspheres.

detecting concentrations of organic solvent, polymer and surfactant were established. Then, Raman spectroscopy and FBRM G400 were used for analyzing dynamic parameters and identifying endpoint of solidification process. Therefore, the application of PAT in this study is helpful for understanding the capability of process and manage the risks caused by sources of variability.

Overall, this study provides novel insights on PLGA development from industrial perspective, which improve robustness, reliability, traceability, batch flexibility and scalability. It can be expected that the application of semi-continuous manufacturing and the establishment of real-time process control loop would significantly accelerate QbD thinking into PLGA microspheres development.

Data availability

The data used to support the findings of this study are available from the corresponding author upon request.

Funding source

This work was supported by Xinjiang Key Laboratory of Active Components and Drug release Technology of Natural drugs (XJDX1713), Xinjiang Medical University Doctoral Research Initiation Fund (201915), and Natural Science Foundation of Xinjiang Uygur Autonomous Region (2021D01C259).

Declaration of competing interest

The authors declare that there are no conflicts of interest regarding the publication of this paper.

Acknowledgements

I would like to show my deepest gratitude to my tutor, Dr. Mubarak Iminjan and Dr. Xun Li a respectable, responsible, and resourceful scholar, and show my gratitude for Ferring Product Development China, Global R&D life cycle management department, Ferring Pharmaceuticals (Asia) Company, they have provided me with valuable guidance and satisfactory experimental condition in every stage of the writing of this manuscript.

References

[1] X. Li, Y. Wei, P. Lv, et al., Preparation of ropivacaine loaded PLGA microspheres as controlled-release system with narrow size distribution and high loading efficiency, Colloids Surf. A Physicochem. Eng. Asp. 562 (2019) 237–246.
[2] X. Li, Z. Zhang, A. Harris, et al., Bridging the gap between fundamental research and product development of long acting injectable PLGA microspheres, Expet Opin. Drug Deliv. (2022) 1–18.
[3] H. Jin, H. Chong, Y. Zhu, et al., Preparation and evaluation of amphipathic lipopeptide-loaded PLGA microspheres as sustained-release system for AIDS prevention, Eng. Life Sci. 20 (11) (2020) 476–484.
[4] K. Wen, X. Na, M. Yuan, et al., Preparation of novel ropivacaine hydrochloride-loaded PLGA microspheres based on post-loading mode and efficacy evaluation, Colloids Surf. B Biointerfaces 210 (2022), 112215.
[5] W. Xu, M. Guo, J. Liu, et al., Poly (lactic-co-glycolic acid)/polycaprolactone nanofibrous membranes for high-efficient capture of nano-and microsized particulate matter, J. Biomed. Nanotechnol. 14 (1) (2018) 179–189.
[6] G.-Q. Zhang, W. Feng, Z. Gao, et al., A NIR ratiometric fluorescent biosensor for sensitive detection and imaging of α-L-fucosidase in living cells and HCC tumor-bearing mice, Aggregate (2022) e286.
[7] X. Li, L.-Z. Xie, J. Li, et al., A pair of new tetrahydro-naphthalenone enantiomers from Eremurus altaicus (Pall.) Stev, Phytochem. Lett. 13 (2015) 330–333.
[8] A. Domokos, B. Nagy, B. Szilagyi, et al., Integrated continuous pharmaceutical technologies—a review, Org. Process Res. Dev. 25 (4) (2021) 721–739.
[9] A.S. Rathore, S. Nikita, G. Thakur, et al., Challenges in process control for continuous processing for production of monoclonal antibody products, Curr. Opin. Chem. Eng. 31 (2021), 100671.
[10] T.C. Silva, M. Eppink, M. Ottens, Automation and miniaturization: enabling tools for fast, high-throughput process development in integrated continuous biomanufacturing, J. Appl. Chem. Biotechnol. 97 (9) (2022) 2365–2375.
[11] Y. Xiao, Q. Liu, X. Tang, et al., Mirror-image thymidine discriminates against incorporation of deoxyribonucleotide triphosphate into DNA and repairs itself by DNA polymerases, Bioconjugate Chem. 28 (8) (2017) 2125–2134.
[12] X. Li, Y. Wei, K. Wen, et al., Novel insights on the encapsulation mechanism of PLGA terminal groups on ropivacaine, Eur. J. Pharm. Biopharm. 160 (2021) 143–151.
[13] A. Butreddy, R.P. Gaddam, N. Kommineni, et al., PLGA/PLA-Based long-acting injectable depot microspheres in clinical use: production and characterization overview for protein/peptide delivery, Int. J. Mol. Sci. 22 (16) (2021) 8884.
[14] Y. Su, B. Zhang, R. Sun, et al., PLGA-based biodegradable microspheres in drug delivery: recent advances in research and application, Drug Deliv. 28 (1) (2021) 1397–1418.
[15] T. Casian, B. Nagy, B. Kovács, et al., Challenges and opportunities of implementing data fusion in process analytical technology—a review, Molecules 27 (15) (2022) 4846.
[16] G. Gerzon, Y. Sheng, M. Kirkitadze, Process analytical technologies–advances in bioprocess integration and future perspectives, J. Pharmaceut. Biomed. Anal. 207 (2022), 114379.
[17] E. Rifna, R. Pandiselvam, A. Kothakota, et al., Advanced process analytical tools for identification of adulterants in edible oils–a review, Food Chem. 369 (2022), 130898.
[18] J. Liu, X. Shen, D. Baimanov, et al., Immobilized ferrous ion and glucose oxidase on graphdiyne and its application on one-step glucose detection, ACS Appl. Mater. Interfaces 11 (3) (2018) 2647–2654.
[19] C. Xiang, Y. Xiao, Z. Ma, et al., Liver resection for large and huge hepatocellular carcinoma: predictors of failure, recurrence patterns, and prognoses, Asia Pac. J. Clin. Oncol. 19 (2) (2022) e60–e70.
[20] Y. Xiao, X. Li, J. Mao, et al., Reverse anti-breast cancer drug resistance effects by a novel two-step assembled nano-celastrol medicine, Nanoscale 14 (21) (2022) 7856–7863.
[21] H. Lv, X. Chen, X. Wang, et al., A novel study on a micromixer with Cantor fractal obstacle through grey relational analysis, Int. J. Heat Mass Tran. 183 (2022), 122159.

[22] J. Schiffbauer, G. Ganchenko, N. Nikitin, et al., Novel electroosmotic micromixer configuration based on ion-selective microsphere, Electrophoresis 42 (23) (2021) 2511–2518.
[23] N. Li, Z. Zhao, H. Ma, et al., Optimization and characterization of low-molecular-weight chitosan-coated baicalin mPEG-PLGA nanoparticles for the treatment of cataract, Mol. Pharm. 19 (11) (2022) 3831–3845.
[24] J. Mo, X. Da, Q. Li, et al., The study of exosomes-encapsulated mPEG-PLGA polymer drug-loaded particles for targeted therapy of liver cancer, J. Oncol. 2022 (2022).
[25] X. Li, Y. Wei, G. Ma, et al., Recent research and development prospects for sustained-release microspheres, J. Beijing Univ. Chem. Technol. 44 (6) (2017) 1.
[26] V. Davydov, E. Roginskii, Y. Kitaev, et al., Phonons in short-period gan/aln superlattices: group-theoretical analysis, ab initio calculations, and raman spectra, Nanomaterials 11 (2) (2021) 286.
[27] A. Arkin, A. Elham, A. Anwar, et al., Optimization and evaluation of the quercus infectoria galls thermosensitive in situ gel for rectal delivery, Evid. base Compl. Alternative Med. (2022) 2022.
[28] A. Elham, M. Arken, G. Kalimanjan, et al., A review of the phytochemical, pharmacological, pharmacokinetic, and toxicological evaluation of Quercus Infectoria galls, J. Ethnopharmacol. 273 (2021), 113592.
[29] J.M. Macharia, R.W. Mwangi, N. Rozmann, et al., Medicinal plants with anti-colorectal cancer bioactive compounds: potential game-changers in colorectal cancer management, Biomed. Pharmacother. 153 (2022), 113383.
[30] X. Rui, S. Jing, Z. Shijiao, et al., Preparation of monodisperse YSZ ceramic microspheres by high-throughput and instant-mixing droplet microfluidic system, Ceram. Int. 47 (13) (2021) 18230–18237.
[31] H. Jayan, H. Pu, D.-W. Sun, Recent developments in Raman spectral analysis of microbial single cells: techniques and applications, Crit. Rev. Food Sci. Nutr. 62 (16) (2022) 4294–4308.
[32] Q. Liu, L. Chen, Z. Zhang, et al., PH-dependent enantioselectivity of D-amino acid oxidase in aqueous solution, Sci. Rep. 7 (1) (2017) 1–9.
[33] O. Geiss, I. Bianchi, C. Senaldi, et al., Particle size analysis of pristine food-grade titanium dioxide and E 171 in confectionery products: interlaboratory testing of a single-particle inductively coupled plasma mass spectrometry screening method and confirmation with transmission electron microscopy, Food Control 120 (2021), 107550.
[34] P. Sagmeister, R. Lebl, I. Castillo, et al., Advanced real-time process analytics for multistep synthesis in continuous flow, Angew. Chem. Int. Ed. 60 (15) (2021) 8139–8148.
[35] D. Panigrahi, P.K. Sahu, S. Swain, et al., Quality by design prospects of pharmaceuticals application of double emulsion method for PLGA loaded nanoparticles, SN Appl. Sci. 3 (6) (2021) 1–21.
[36] M. Zeeshan, H. Ali, Q.U. Ain, et al., A holistic QBD approach to design galactose conjugated PLGA polymer and nanoparticles to catch macrophages during intestinal inflammation, Mater. Sci. Eng. C 126 (2021), 112183.
[37] B. Bai, Y. Liu, Q. Wang, et al., Experimental investigation on gasification characteristics of plastic wastes in supercritical water, Renew. Energy 135 (2019) 32–40.
[38] T. Tolcha, T. Gemechu, S. Al-Hamimi, et al., Multivariate optimization of a combined static and dynamic supercritical fluid extraction method for trace analysis of pesticides pollutants in organic honey, J. Separ. Sci. 44 (8) (2021) 1716–1726.
[39] P.-S. Wei, Y.-J. Chen, S.-Y. Lin, et al., In situ subcutaneously injectable thermosensitive PEG-PLGA diblock and PLGA-PEG-PLGA triblock copolymer composite as sustained delivery of bispecific anti-CD3 scFv T-cell/anti-EGFR Fab Engager (BiTEE), Biomaterials 278 (2021), 121166.
[40] S.-L. Bee, Z.A. Hamid, M. Mariatti, et al., Approaches to improve therapeutic efficacy of biodegradable PLA/PLGA microspheres: a review, Polym. Rev. 58 (3) (2018) 495–536.
[41] S. Ding, C.A. Serra, T.F. Vandamme, et al., Double emulsions prepared by two–step emulsification: history, state-of-the-art and perspective, J. Contr. Release 295 (2019) 31–49.
[42] M. Ali, X.F. Walboomers, J.A. Jansen, et al., Influence of formulation parameters on encapsulation of doxycycline in PLGA microspheres prepared by double emulsion technique for the treatment of periodontitis, J. Drug Deliv. Sci. Technol. 52 (2019) 263–271.